



# miR-185-5p / ATG101 axis alleviated intestinal barrier damage in intestinal ischemia reperfusion through autophagy

Wendong Chen, Li Ma, Jianlin Shao, Chun Bi, Junjie Li, Wei Yang\*

Department of Anesthesiology, The First Affiliated Hospital of Kunming Medical University, Kunming 650032, Yunnan Province, China

## ARTICLE INFO

### Keywords:

miR-185-5p  
Intestinal ischemia reperfusion  
Autophagy  
Intestinal barrier damage  
ATG101

## ABSTRACT

**Objective:** Intestinal ischemia-reperfusion (II/R) is a common pathological injury in clinic, and the systemic inflammatory response it causes will lead to multiple organ damage and functional failure. miR-185-5p has been reported to be a regulator of inflammatory response and autophagy, but whether it participates in the regulation of autophagy in II/R is still unclear. Therefore, we aimed to explore the mechanism of miR-185-5p regulating intestinal barrier injury in (II/R).

**Methods:** Caco-2 cells was induced by oxygen-glucose deprivation/reoxygenation (OGD/R) to establish II/R model. The superior mesenteric artery of C57BL/6 mice was clamped for 45 min and then subjected to reperfusion for 4 h for the establishment of II/R mice model. miR-185-5p mimic, miR-185-5p inhibitor, pcDNA-autophagy-related 101 (ATG101) were respectively transfected into Caco-2 cells. Real-time quantitative polymerase chain reaction (RT-qPCR) was performed to assess miR-185-5p expression. Western blot detected the level of ATG101 and tight junction-associated proteins ZO1, Occludin, E-cadherin,  $\beta$ -catenin, as well as autophagy markers ATG5, ATG12, LC3I/II, Beclin1 and SQSTM1. Transepithelial electrical resistance (TEER) values was detected by a resistance meter. FITC-Dextran was performed to measure cell permeability. 5-ethynyl-2'-deoxyuridine (EDU) staining measured cell proliferation. Transmission electron microscope was conducted to observe autophagosomes. Hematoxylin & eosin (H&E) staining observed the damage of mice intestinal. Immunohistochemistry (IHC) measured the percentage of ki67 positive cells. TdT-mediated dUTP nick-end labeling (TUNEL) assay assessed cell apoptosis in intestinal tissues of II/R. Dual-luciferase assay verified the targeting relationship between miR-185-5p and ATG101.

**Results** miR-185-5p was overexpressed in OGD/R-induced Caco-2 cells and intestinal tissues of II/R mice. Knocking down miR-185-5p markedly promoted autophagy and TEER values, reduced cell permeability, and alleviated intestinal barrier damage. ATG101 was a target of miR-185-5p, and overexpression of ATG101 promoted autophagy and dampened OGD/R-induced intestinal barrier damage. Overexpression of miR-185-5p reversed the effect of overexpressed ATG101 on OGD/R-induced Caco-2 cells.

**Conclusion:** Knockdown of miR-185-5p enhanced autophagy and alleviated II/R intestinal barrier damage by targeting ATG101.

\* Corresponding author. Department of Anesthesiology, The first affiliated hospital of Kunming medical University, No.295 Xichang Rd, Kunming 650032, Yunnan Province, China

E-mail address: [yangwei1@ydy.cn](mailto:yangwei1@ydy.cn) (W. Yang).

<https://doi.org/10.1016/j.heliyon.2023.e18325>

Received 16 March 2023; Received in revised form 12 July 2023; Accepted 13 July 2023

Available online 16 July 2023

2405-8440/© 2023 The Authors. Published by Elsevier Ltd. This is an open access article under the CC BY-NC-ND license (<http://creativecommons.org/licenses/by-nc-nd/4.0/>).

## 1. Introduction

Intestinal ischemia-reperfusion (II/R) is a pathological injury caused by sepsis, hemorrhagic shock, intestinal obstruction and other factors [1,2]. In the early stage of II/R injury, it may cause severe intestinal epithelial damage, resulting in local inflammation and loss of intestinal barrier function. Subsequent reperfusion injury triggers a systemic inflammatory response that leads to multiple organ damage and functional failure [3,4]. Intestinal epithelial barrier is composed of intestinal epithelial cells and the tight junction between epithelial cells and biofilm. It is also an important mechanical barrier in the intestinal mucosal barrier, which can effectively prevent bacteria, endotoxin and other harmful substances from entering the blood through the intestinal mucosa [5]. Tight junction is a protein complex composed of transmembrane proteins, which is located at the top of epithelial cell membrane [6,7]. It has been reported that the expression of tight junction-related proteins is closely related to the intestinal barrier function [8]. Therefore, it is vital to study the mechanism of intestinal barrier dysfunction for the diagnosis and treatment of II/R injury.

Mitochondrial autophagy is a process that selectively recognizes and eliminates damaged mitochondria, which plays a role in maintaining the normal function of mitochondria and is involved in the regulation of a variety of physiological and pathological processes in the body [9,10]. Recently, more and more reports have shown that autophagy regulate the occurrence and development of tumors [11], bone injuries [12], neurological diseases [13] and a variety of inflammatory response-related diseases [14,15]. II/R is a typical inflammatory disease. Studies have shown that autophagy not only play a protective role in intestinal mucosal dysfunction caused by II/R injury, but also promote the destruction of intestinal mucosal barrier [16,17]. Chen et al. [18] revealed that activating autophagy through ischemic postconditioning ameliorated II/R injury. However, Li et al. [19] reported that inhibition of autophagy reduced the intestinal damage in II/R mice. Therefore, it is necessary to further study the molecular mechanism of regulating autophagy in II/R.

miRNAs are non-coding RNAs which has been studied more recently and verified miRNAs are involved in the regulation of cell differentiation, cell proliferation, metastasis, senescence and apoptosis [20]. For instance, miR-421 was overexpressed in non-small cells lung cancer, and enhanced the radiotherapy resistance of A549 cells via inhibiting PTEN [21]. miR-19b-3p promoted inflammation and cell death during cerebral ischemia reperfusion injury through regulating SIRT1/FoxO3/SPHK1 axis [22]. miR-185-5p is a regulator of inflammatory responses, and has been reported to mediate inflammatory responses in macrophages [23], high glucose-induced mouse mesangial cells [24], and myocardial ischemia-reperfusion [25]. Moreover, Yang et al. [26] found that increased miR-185-5p inhibited autophagy and cell growth of non-small cell lung cancer. Liu et al. [27] also reported miR-185-5p inhibited the autophagy level in colorectal cancer. However, the regulatory mechanism of miR-185-5p in II/R mediated by autophagy remains unclear.

In the current study, we explored the effect of miR-185-5p on II/R intestinal barrier through cellular and *in vivo* experiments, respectively, and predicted the potential target genes of miR-185-5p through the starbase database. Studies found that the expression of miR-185-5p was increased in oxygen-glucose deprivation/reoxygenation (OGD/R)-stimulated Caco-2 cells and II/R-induced mouse intestinal tissue, knocking down miR-185-5p increased autophagy and relieved intestinal barrier damage in II/R by upregulating ATG101.

## 2. Materials and methods

### 2.1. Cell culture and treatment

Human colorectal cancer cell Caco-2 was purchased from Wuhan Procell (China), Ltd. Caco-2 cells were grown in MEM medium (Containing 20% FBS and 1% Penicillin and streptomycin) (Procell, Wuhan, China) and placed in a cell incubator at 37 °C and 5% CO<sub>2</sub>. The II/R model cells were induced by OGD/R. Caco-2 cells were cultured in MEM medium without glucose for 12 h. Subsequently, the cells recovered oxygen for 0 h, 6 h and 12 h, respectively. The expression of miR-185-5p in the cells was detected by PCR.

### 2.2. Cell transfection

miR-185-5p mimic, miR-185-5p inhibitor, ago-miR-185-5p, antago-miR-185-5p, pcDNA-ATG101 and the corresponding negative control were synthesized by Genomeditech (Shanghai, China). Then the transfection was performed by Lipofectamine 2000 (Thermo Fisher Scientific, Waltham, MA, USA) according to the instruction. 12.5 nmol Rapamycin were used to treat Caco-2 cells transfected with miR-185-5p inhibitor, and 2.5 nmol 3-Methyladenine (3-MA, an autophagy inhibitor) were used to treat Caco-2 cells transfected with miR-185-5p inhibitor and pcDNA-ATG101. Subsequently, that cells were stimulated by OGD/R.

**Table 1**  
Primer sequences.

Target	Primer sequences (F: Forward primer. R: Reverse primer)
miR-185-5p	F 5'-TGGAGAGAAAGGCAGTTCCTG-3' R 5'-CAGGCGGTCTGGAGT-3'
U6	F 5'-CTCGCTTCGGCAGCAC-3' R 5'-AACGCTTCACGAATTTGCGT-3'

### 2.3. Real-time quantitative polymerase chain reaction (RT-qPCR)

The total RNA in the cells was extracted and reverse transcribed into cDNA using a reverse transcription kit (Qiagen, Duesseldorf, Germany). The PCR reaction was performed on a fluorescence quantitative instrument using the TB Green™ Premix Ex Taq™ II kit (Takaya, Japan). The reaction conditions were as follows: pre-denaturation at 94 °C for 2 min, denaturation at 94 °C for 15 s, annealing at 60 °C for 15 s and extensions at 72 °C for 10 s, a total of 40 cycles was performed. The relative expression of the target gene was calculated by  $2^{-\Delta\Delta Ct}$ . Table 1 displayed the primer sequences.

### 2.4. Ethynyldeoxyuridine (EDU)

The cells were inoculated into the 24-well plate, and EDU working solution (RiBoBio, Guangzhou, China) was prepared, preheated, and added into the 24-well plate to incubate with the cells for 2 h. The cell culture medium was removed, and immunostaining fixative liquid was added into the well plate. After 15 min, glycine was added to incubate the cells for 5 min. Subsequently, the cells were incubated with 0.5% Triton X-100 osmotic agent, Apollo and Hoechst 33342 staining solutions, respectively. Fluorescence microscope was performed to take photo.

### 2.5. Transepithelial electrical resistance (TEER) measurements

The TEER value was detected using a microcellular resistance system. The cells in incubator were taken out and placed at room temperature for 30 min. After the culture medium was removed, a new cell culture medium was added and the TEER value was measured.  $TEER (\Omega \cdot cm^2) = (\text{Sample resistance value} - \text{blank control value}) \times \text{Membrane surface area of Transwell chamber}$ .

### 2.6. Cell permeability detection

The Caco-2 cells were inoculated into the upper chamber of Transwell (Corning Incorporated, Corning, NY, USA), and  $3 \times 10^4$  cells per well were cultured for 24 h. 10 mg/mL FITC-Dextran (MedchemExpress, Monmouth Junction, NJ, USA) was added to the upper chamber for incubation. 2 h later, the cell culture medium was collected, and the absorbance value was detected by a microplate reader (Thermo Fisher Scientific, Waltham, MA, USA).

### 2.7. Experimental animals

Twenty-four male C57BL/6 mice (20–22 g) were purchased from SPF (Beijing, China) Biotechnology Co., Ltd (SCXK (Jing) 2019-0010). The mice were adaptively fed for one week after purchase, and they were freely accessed to food and water. This study was approved by the Laboratory Animal Ethics Committee of Yunnan Laberal Biotechnology co., Ltd (PZ20220413).

### 2.8. Establishment of II/R

The mice were randomly divided into four groups (sham group, II/R group, ago-miR-185-5p group, antago-185-5p group), with six mice in each group. After the mice were anesthetized, the mice (II/R group, ago-miR-185-5p group, antago-185-5p group) were opened the abdominal cavity, clamped the superior mesenteric artery for 45 min, and then made reperfusion for 4 h. Mice in the ago-miR-185-5p group were injected with ago-miR-185-5p through tail vein for three consecutive days, and antago-miR-185-5p group mice were injected with antago-miR-185-5p through tail vein for three consecutive days, then the mice were treated with II/R. In the sham group, mice were injected with the same amount of normal saline, and their abdomen was slit and then sutured without II/R treatment. After the experiment, the mice were euthanized and samples were taken.

### 2.9. Immunofluorescence (IF)

Paraffin sections were dewaxed, dehydrated in a gradient of alcohol, and subjected to antigen repair. After 10 min, 3% BSA reagent was added dropwise for blocking. After 30 min, the primary antibody (Abcam, Shanghai, China) and secondary antibody (Abcam, Shanghai, China) were added dropwise on the section samples respectively. DAPI reagent was added to stain the nuclei after rinsing. Fluorescence microscope was applied to observe and take pictures.

### 2.10. Western blot

The transfected cells were collected from each group and total protein was extracted using RIPA reagent. The BCA protein quantitative kit (Beyotime, Shanghai, China) determined the concentration of protein. SDS-PAGE gel electrophoresis separated the protein, then the protein was transferred to PVDF membranes (Beyotime, Shanghai, China). After being rinsed with TBST, 5% blocking solution was added to block the membrane for 1 h, and the membrane was incubated with the diluted primary antibody (Abcam, Shanghai, China) overnight, the secondary antibody (Abcam, Shanghai, China) was added and incubated for 1 h. After treatment with the ECL luminescent liquid (Yuanye Bio-Technology, Shanghai, China), the chemical imager was performed to display images.

2.11. Luciferase report gene assay

Starbase database predicted the targeted binding sites of miR-185-5p and ATG101, and simultaneously constructed and amplified the mutation sequence of ATG101 onto a pmirGLO vector to obtain wild-type (WT) and mutant (MUT) vectors of ATG101 (pmirGLO-ATG101-WT/MUT). miR-185-5p mimic and pmirGLO-ATG101-WT/MUT were respectively transfected into Caco-2 cells. Culture in a cell incubator for 48 h. According to the instructions, dual-luciferase reporter kit (Thermo Fisher Scientific, Waltham, MA, USA) was used to assess the luciferase activity.

2.12. Hematoxylin & eosin (HE) assay

The paraffin sections were placed in an oven at 60 °C for 2 h, deparaffinized with xylene and ethanol and rinsed with distilled water. The sections were stained in hematoxylin solution for 3 min, and reacted with hydrochloric acid ethanol until the nuclei were blue. Subsequently, the sections were added with eosin, rinsed with distilled water after 2 min, and dehydrated with gradient ethanol. The slices were sealed and observed under a microscope.

2.13. Intestinal permeability of mice

FITC-dextran was used to evaluated intestinal permeability of mice. Briefly, 30 min before anesthetized, 0.6 mg/g FITC-dextran (MedchemExpress, Monmouth Junction, NJ, USA) was intragastrically administered to the mice. The blood was collected by cardiac puncture after 30 min. The intensity of FITC-dextran was measured at 520 nm.

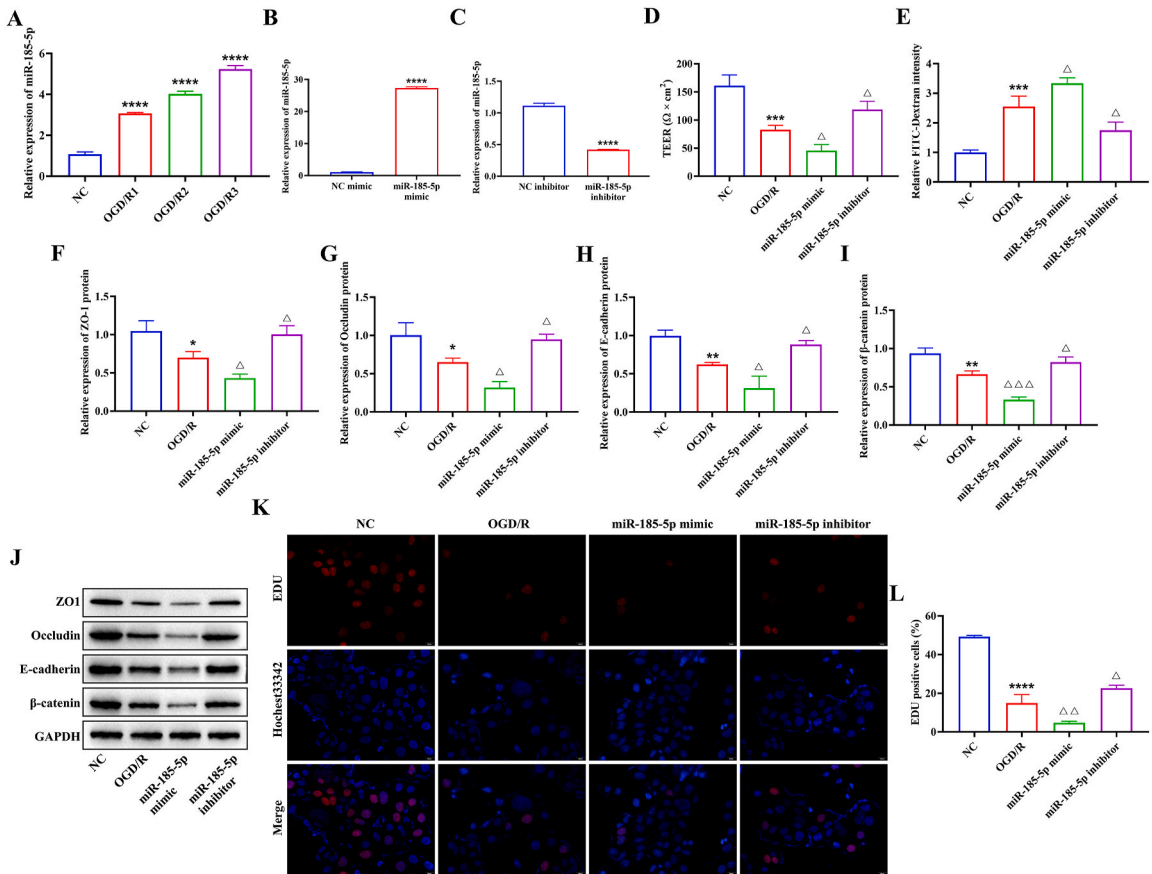


**Fig. 1. miR-185-5p mediated the II/R.** A RT-qPCR was performed to assess the level of miR-185-5p. B and C RT-qPCR detected the transfected efficiency of miR-185-5p mimic and miR-185-5p inhibitor. D Measurements of TEER. E Cell permeability was investigated through FITC-dextran. F-J Western blot was used to assess the tight junction-associated proteins ZO-1, Occludin, E-cadherin and β-catenin expression. K EDU assay detected cell proliferation rate. \**P* < 0.05, \*\**P* < 0.01, \*\*\**P* < 0.001, \*\*\*\**P* < 0.0001 vs. NC group. Δ*P* < 0.05, ΔΔ*P* < 0.01, ΔΔΔ*P* < 0.001 vs. OGD/R group.



2.14. Immunohistochemical (IHC) assay

The intestinal tissues of mice were embedded in paraffin and sectioned. The tissues were deparaffinized by xylene and gradient ethanol, and the antigen was repaired by sodium citrate. 0.5% Triton-100 was added dropwise onto the tissue sections, rinsed, blocked with 3% fetal bovine serum, incubated overnight with the primary antibody (Abcam, Shanghai, China), and incubated with the secondary antibody (Abcam, Shanghai, China) at room temperature for 2 h. After staining with DAB and hematoxylin respectively, the sections were dehydrated and sealed. Observation and staining under a microscope.

2.15. TdT-mediated dUTP nick-end labeling (TUNEL)

The paraffin-embedded mice intestinal tissues were sectioned, dewaxed and treated with protease K working solution for 30 min. After washing with PBS, 50 μL TUNEL reaction solution (Beyotime, Shanghai, China) was added to react in the dark for 1 h, followed by washing with PBS and sealing with anti-fluorescence quencher. The staining results were observed under fluorescence microscope.

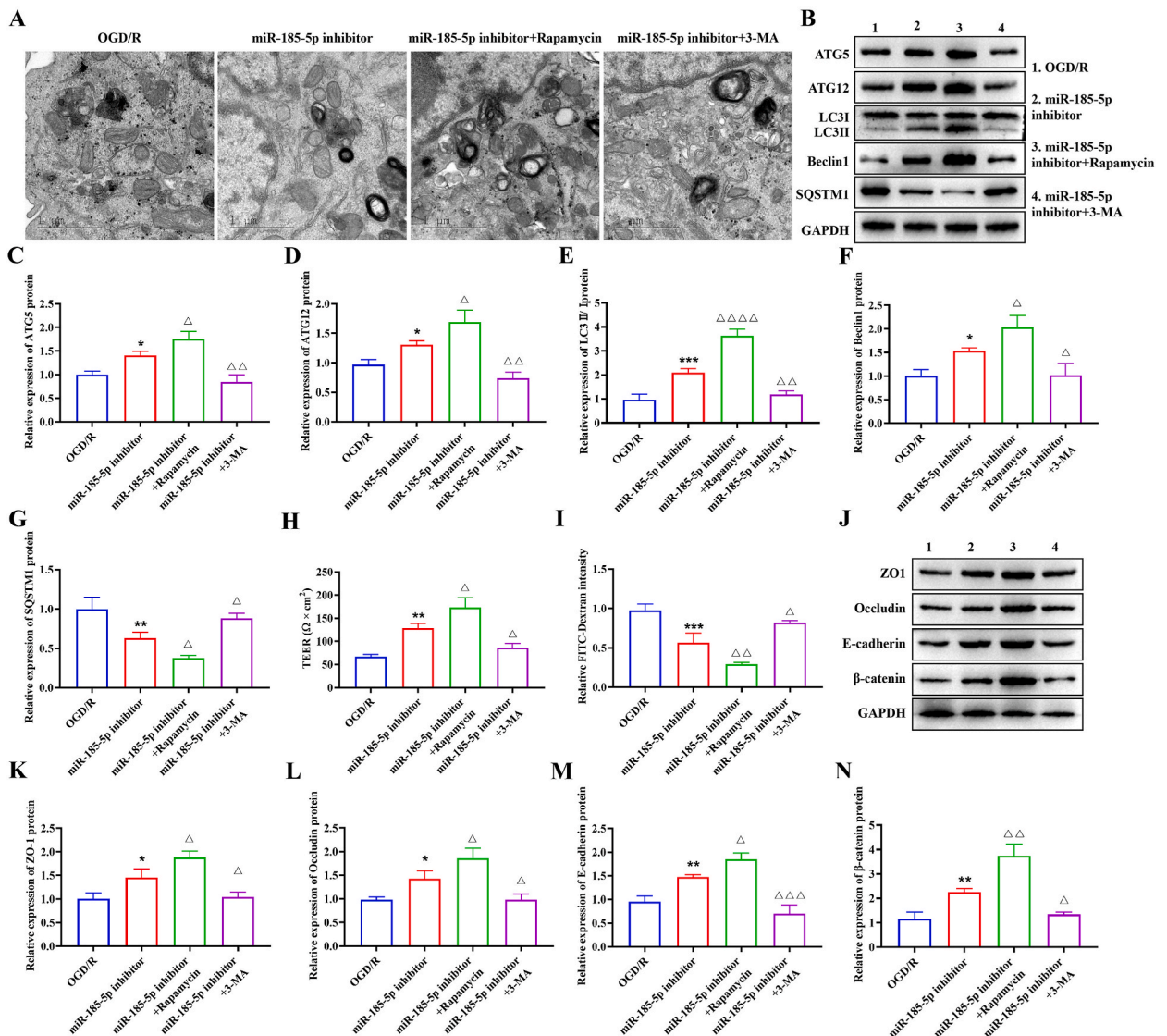


**Fig. 2. miR-185-5p regulated II/R mediated by autophagy.** A Transmission electron microscope was used to observe the autophagosome. B-G Western blot was utilized to detect the level of autophagy markers ATG5, ATG12, LC3I/II, Beclin1, SQSTM1 protein. H Measurements of TEER. I Cell permeability was investigated through FITC-dextran. J-N Western blot assessed the level of ZO-1, Occludin, E-cadherin and β-catenin. \*P < 0.05, \*\*P < 0.01, \*\*\*P < 0.001 vs. OGD/R group.  $\Delta$ P < 0.05,  $\Delta\Delta$ P < 0.01 vs. miR-185-5p inhibitor group.

2.16. Statistical analyze

The above experiments were repeated three times. The data was displayed as mean ± standard deviation. GraphPad Prism 8.0 software was performed to analyze the data. Unpaired student's *t*-test assessed the difference between two groups. Statistical significance among multiple groups was examined by One-way ANOVA. P value less than 0.05 was considered statistically significant.

3. Results

3.1. miR-185-5p mediated the II/R damage

We induced the II/R cell model through OGD/R. Caco-2 cells were treated with oxygen-glucose deprivation for 12 h, and then

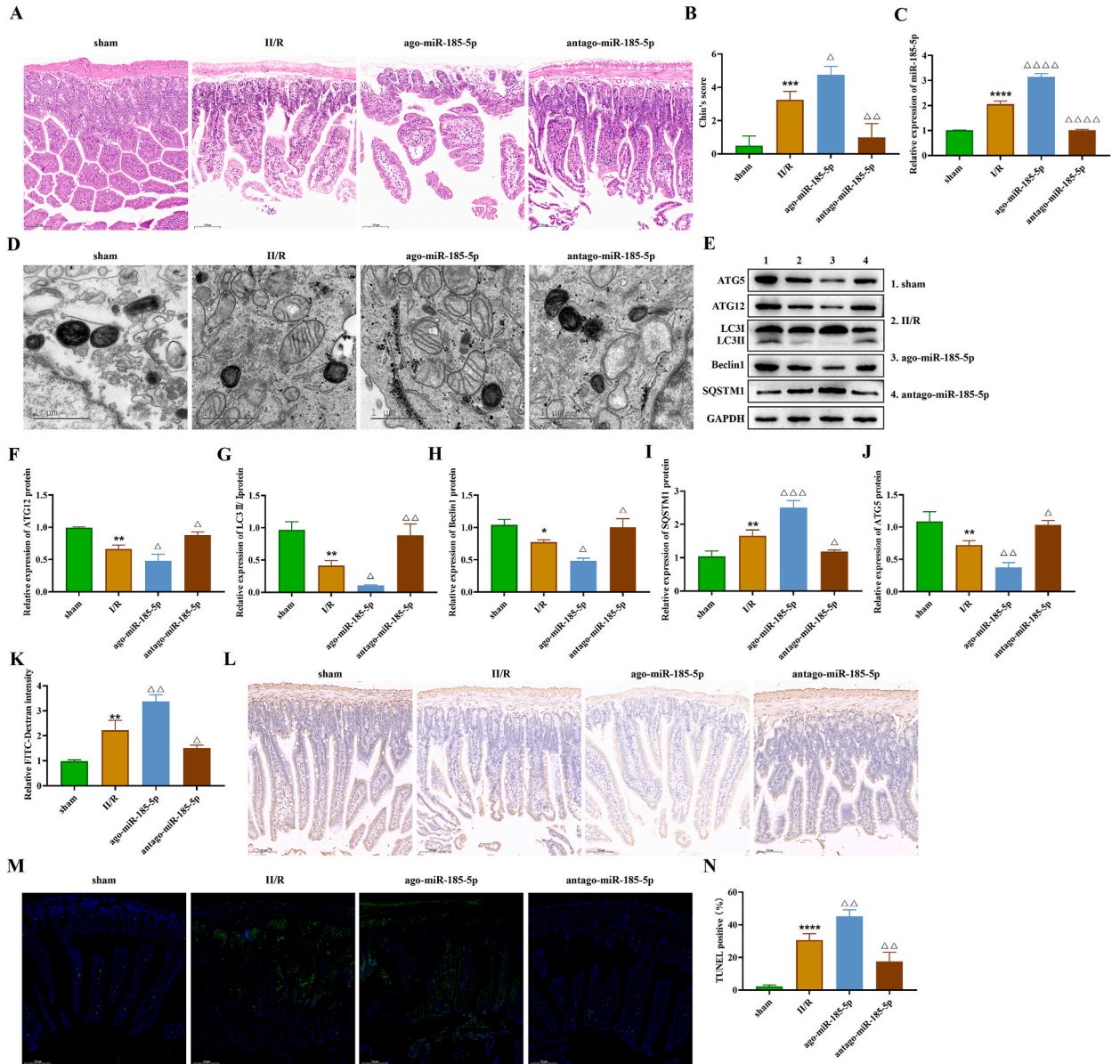


**Fig. 3.** miR-185-5p regulated intestinal barrier damage *in vivo*. A HE staining observed the intestinal damage. B Chiu's score of intestinal in intestinal damage mice. C RT-qPCR measured the expression of miR-185-5p. D Transmission electron microscope observed the autophagosome. E-J Western blot determined the protein level of ATG5, ATG12, LC3I/II, Beclin1 and SQSTM1 protein. K FITC-dextran evaluated the intestinal permeability of mice. L IHC staining detected the ki67 positive cells. M and N TUNEL staining was applied to assess the apoptosis of cells in tissues. \**P* < 0.05, \*\**P* < 0.01, \*\*\**P* < 0.001, \*\*\*\**P* < 0.0001 vs. sham group.  $\Delta$ *P* < 0.05,  $\Delta\Delta$ *P* < 0.01,  $\Delta\Delta\Delta$ *P* < 0.001 vs. II/R group.

reoxygenated for 0 h, 6 h, 12 h. RT-qPCR results showed that miR-185-5p was increased with the increase of reoxygenate time (Fig. 1A). And we selected 6 h as the reoxygenate time for the future study. To investigate the mechanism of miR-185-5p in II/R, miR-185-5p mimic, miR-185-5p inhibitor and the corresponding negative control was respectively transfected into Caco-2 cells, then treated Caco-2 cells with OGD/R. miR-185-5p expression in miR-185-5p mimic group was overexpressed (Fig. 1B), and downregulated in miR-185-5p inhibitor group (Fig. 1C).

TEER and permeability detection revealed that treatment with OGD/R inhibited the TEER values (Fig. 1D) and increased the flux of FITC-dextran (Fig. 1E). Upregulated miR-185-5p inhibited TEER values and stimulated the flux of FITC-dextran than those in OGD/R group. Knocking down miR-185-5p alleviated the effect of OGD/R on Caco-2 cells. Furthermore, Western blot (Fig. 1F–J) and EDU assay (Fig. 1K–L) displayed tight junction-associated proteins ZO1, Occludin, E-cadherin,  $\beta$ -catenin levels and cell proliferation were obviously decreased in the OGD/R groups. Compared with OGD/R group, overexpression of miR-185-5p promoted the influence of OGD/R on Caco-2 cells. Decreased miR-185-5p activated ZO1, Occludin, E-cadherin,  $\beta$ -catenin expression and proliferation rate than those in OGD/R group. Therefore, upregulation of miR-185-5p enhanced the intestinal barrier injury in OGD/R-stimulated Caco-2 cells.

### 3.2. miR-185-5p regulated II/R mediating by autophagy

It has been reported that autophagy participated in the regulation of intestinal barrier injury [28], thus we attempted to explore whether the regulation of intestinal barrier damage by miR-185-5p was mediated by autophagy. We treated Caco-2 cells with autophagy activator Rapamycin and inhibitor 3-MA after transfection of miR-185-5p inhibitor. The experimental revealed the number of autophagosomes (Fig. 2A) and the expression of the autophagy markers (Fig. 2B) ATG5 (Fig. 2C), ATG12 (Fig. 2D), LC3II/I (Fig. 2E) and Beclin1 (Fig. 2F) were rose, but SQSTM1 (Fig. 2G) was downregulated in the miR-185-5p inhibitor group. Rapamycin enhanced autophagy level stimulated by miR-185-5p inhibitor, while 3-MA dampened the level of autophagy than those in miR-185-5p inhibitor group. What's more, compared with knockdown of miR-185-5p group, Rapamycin increased the values of TEER (Fig. 2H), dampened the flux of FITC-dextran (Fig. 2I), and promoted the level of ZO1 (Fig. 2J–K), Occludin (Fig. 2L), E-cadherin (Fig. 2M) and  $\beta$ -catenin (Fig. 2N). 3-MA diminished the effect of miR-185-5p inhibitor on intestinal barrier damage (Fig. 2H–N). In conclusion, miR-185-5p inhibited autophagy level, then stimulated the intestinal barrier damage in II/R.

### 3.3. miR-185-5p mediated intestinal barrier damage in vivo

Next, we will discuss the regulation of miR-185-5p on intestinal II/R *in vivo*. Histological evaluation results showed that the intestinal mucosal structure of mice in the sham group was normal (Fig. 3A), and the intestinal mucosal structure of mice in the II/R group was significantly damaged. The damage in the ago-miR-185-5p group was serious than that in the II/R group. Mild injury in antago-miR-185-5p was seen. Ago-miR-185-5p increased Chiu's score (Fig. 3B) and miR-185-5p expression (Fig. 3C), while antago-

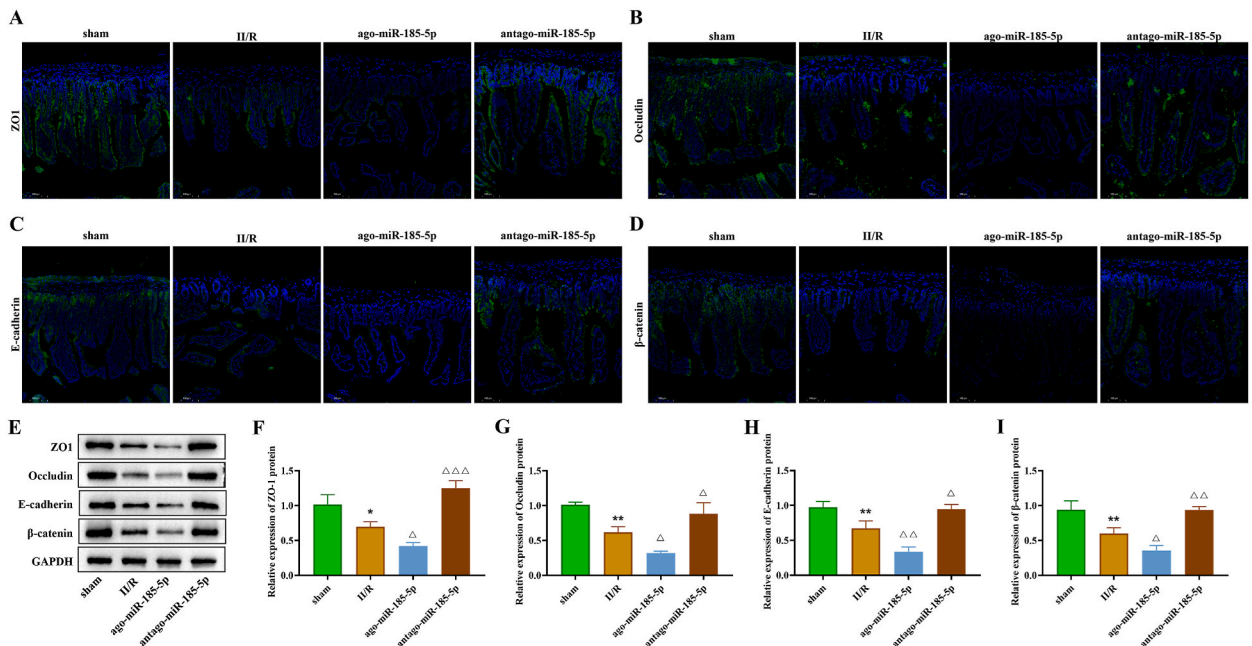


**Fig. 4.** miR-185-5p regulated tight junction-associated proteins in II/R mice. IF staining was used to detect the fluorescence intensity of ZO1 (A), Occludin (B), E-cadherin (C) and  $\beta$ -catenin (D). E–I The protein expression of ZO1, Occludin, E-cadherin and  $\beta$ -catenin was detected by Western blot. \*P < 0.05, \*\*P < 0.01 vs. sham group.  $\Delta$ P < 0.05,  $\Delta\Delta$ P < 0.01,  $\Delta\Delta\Delta$ P < 0.001 vs. II/R group.



miR-185-5p decreased Chiu's score and inhibited the level of miR-185-5p. Ago-miR-185-5p reduced autophagosome numbers (Fig. 3D) and ATG5 (Fig. 3E and F), ATG12 (Fig. 3G), LC3II/I (Fig. 3H), Beclin1 (Fig. 3I) expression, promoted SQSTM1 expression (Fig. 3J) and the intestinal permeability of mice after II/R injury. The autophagosome numbers and proteins level of ATG5, ATG12, LC3II/I, Beclin1 in antago-miR-185-5p group mice was rose, SQSTM1 level and the intestinal permeability was lower than II/R group. IHC and TUNEL results verified that ago-miR-185-5p reduced the percentage of ki67 positive cells (Fig. 3L) and upregulated TUNEL positive cells (Fig. 3M and N) in intestinal tissues, while antago-miR-185-5p had the opposite result.

IF (Fig. 4A–D) and Western blot (Fig. 4E–I) measurements revealed the fluorescence intensity and proteins expression of ZO1, Occludin, E-cadherin and  $\beta$ -catenin in ago-miR-185-5p group was dampened, antago-miR-185-5p increased their fluorescence intensity and proteins level. To sum up, overexpressed miR-185-5p aggravated intestinal injury in intestinal II/R mice through attenuating autophagy.

### 3.4. ATG101 was a target of miR-185-5p

To study the specific regulatory mechanism of miR-185-5p in intestinal II/R, we used the Starbase database to predict the potential target of miR-185-5p, and found ATG101 3'-untranslated region had binding sequences with miR-185-5p (Fig. 5A). Dual-luciferase reporter assay deeply validated the targeting relationship between miR-185-5p and ATG101 (Fig. 5B). Western lot results showed miR-185-5p mimic downregulated ATG101 (Fig. 5C and D), miR-185-5p inhibitor activated ATG101, and the differences had statistically significant. These results suggested ATG101 acted as a target of miR-185-5p and miR-185-5p negatively regulating the expression of ATG101.

### 3.5. miR-185-5p/ATG101 axis regulated intestinal barrier after OGD/R via autophagy

The above experiments demonstrated miR-185-5p promoted intestinal barrier damage in intestinal II/R by inhibiting autophagy, and miR-185-5p negatively regulated ATG101. Then we will investigate whether ATG101 acts as a protective factor for intestinal barrier damage. Western blot detection showed ATG101 in Caco-2 cells transfected with pcDNA-ATG101 was higher than pcDNA-NC (Fig. 6A and B). pcDNA-ATG101 promotion enhanced the autophagy level (Fig. 6C–I). Upregulated miR-185-5p or treatment with 3-MA diminished the promotion effect of pcDNA-ATG101 on autophagy. Compared with control group, pcDNA-ATG101 rose TEER values (Fig. 6J), attenuated the flux of FITC-dextran (Fig. 6K), as well as upregulated ZO1 (Fig. 6L and M), Occludin (Fig. 6N), E-cadherin (Fig. 6O) and  $\beta$ -catenin (Fig. 6P). pcDNA-ATG101+miR-185-5p mimic group and pcDNA-ATG101+3-MA group decreased the values of TEER, rose the flux of FITC-dextran, and decline ZO1, Occludin, E-cadherin and  $\beta$ -catenin expression than those in

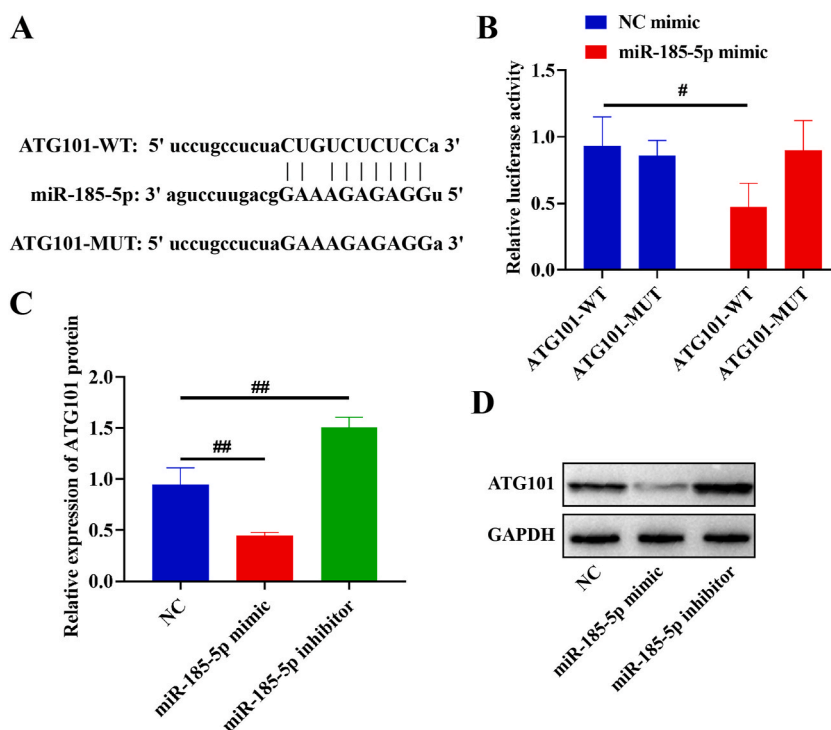


**Fig. 5. miR-185-5p targeted ATG101.** A Starbase database predicted the binding sites of miR-185-5p and ATG101. B Luciferase reporter experiment verified the target relationship between miR-185-5p and ATG101. C and D The protein expression of ATG101 was performed using Western blot. # $P < 0.05$ , ## $P < 0.01$ .

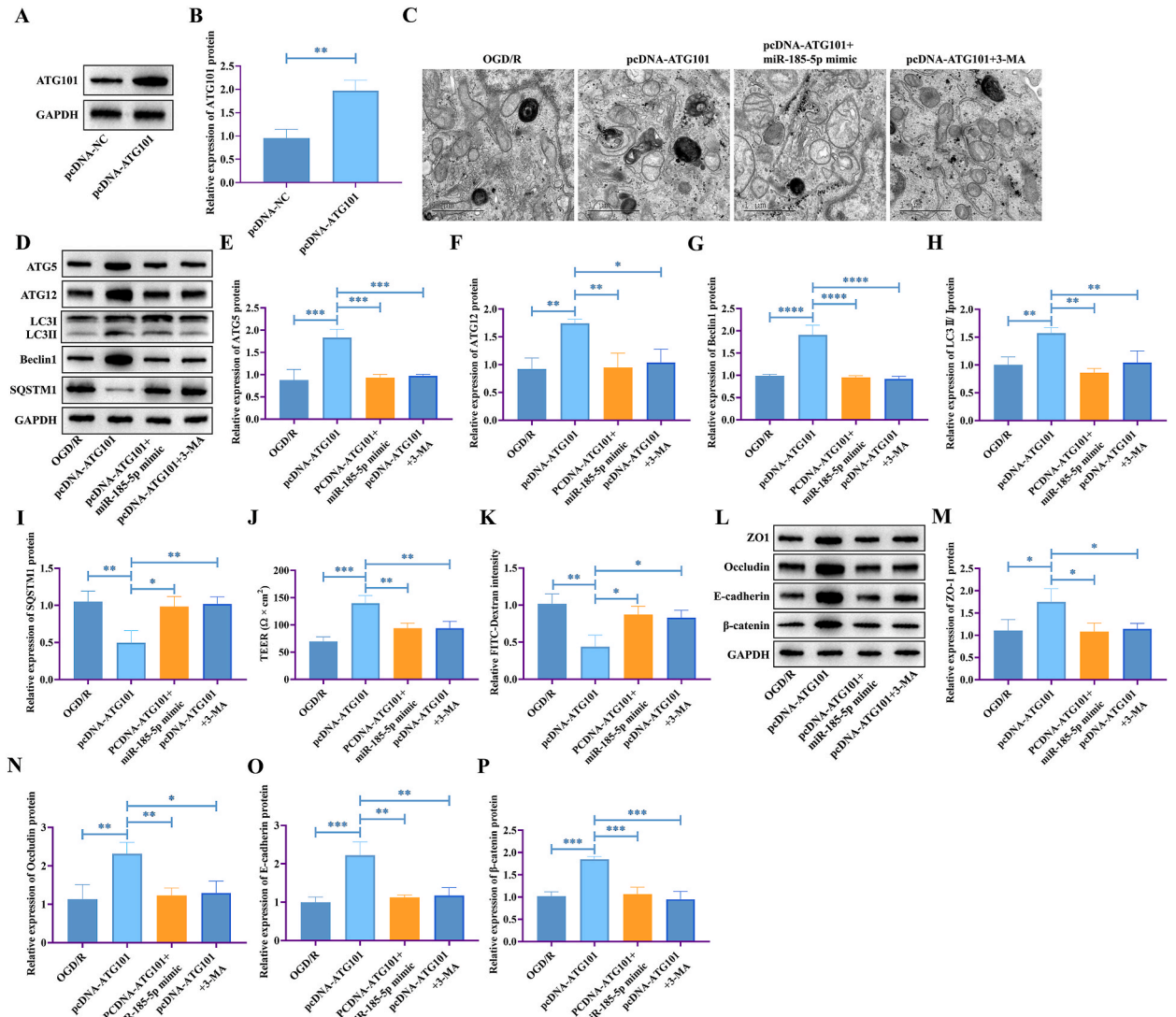


**Fig. 6.** miR-185-5p/ATG101 axis regulated intestinal barrier after OGD/R via autophagy. A and B ATG101 protein level was assessed by Western blot. C The autophagosome was observed by transmission electron microscope. D-I Western blot was used detect ATG5, ATG12, LC3I/II, Beclin1 and SQSTM1 level. J Measurements of transepithelial electrical resistance. K Cell permeability was investigated through FITC-dextran. L-P The expression of ZO1, Occludin, E-cadherin and  $\beta$ -catenin was determined by Western blot. \* $P < 0.05$ , \*\* $P < 0.01$ , \*\*\* $P < 0.001$ , \*\*\*\* $P < 0.0001$ .

pcDNA-ATG101 group (Fig. 6I–O). In conclusion, overexpression of miR-185-5p dampened autophagy, increased the intestinal barrier damage in OGD/R-induced Caco-2 cells through downregulating ATG101.

**4. Discussion**

II/R is a common severe disease in clinic, which may lead to traumatic shock and multiple organ failure in patients, with a high morbidity and mortality rate. Intestinal barrier dysfunction due to the destruction of tight junctions plays a key role in II/R formation. Our study found that miR-185-5p broke tight junction and aggravated intestinal barrier damage in II/R by targeting ATG101 to inhibit autophagy.

Previous studies have found that miRNA is involved in the regulation of the occurrence and development of II/R injury [29–31]. Liu et al. [17] found that overexpressed miR-146a-5p inhibited autophagy and alleviated II/R injury via PRKAA/mTOR pathway by targeting TXNIP. miR-26a-5p enhanced oxidative stress to exacerbate II/R injury by targeting PPAR $\alpha$  [29]. In ischemic post-conditioning, HIF- $\alpha$  reduced II/R injury by promoting miR-21 and inhibiting apoptosis [30]. The low-expression miR-665-3p reduced II/R-induced systemic inflammation and apoptosis by promoting autophagy [31]. What’s more, inhibition of miR-34a-5p [32], miR-351-5p [33], miR-381-3p [5] also been validated relieved II/R damage. In the study, we revealed that miR-185-5p was increased

in OGD/R-induced Caco-2 cells and the intestinal tissues of II/R mice. Knocking down miR-185-5p upregulated the values of TEER and the expression of tight junction-associated protein ZO1, Occludin, E-cadherin and  $\beta$ -catenin, as well as suppressed the permeability in OGD/R-induced Caco-2 cells by promoting autophagy level. Meanwhile, the inhibition of miR-185-5p expression markedly alleviated intestinal barrier injury in mice. Conversely, overexpression of miR-185-5p aggravated intestinal barrier damage in II/R mice by inhibiting autophagy levels.

miR-185-5p has a wide range of regulatory effects and is involved in a variety of physiological processes [34–36]. For example, upregulated miR-185-5p inhibited the inflammation in lipopolysaccharide-stimulated macrophages through MAPK/JNK pathway [23, 37]. miR-185-5p could diminish inflammatory response and pyroptosis in human cardiac myocytes induced by hypoxia/reoxygenation (H/R), therefore alleviated H/R-induced myocardial injury [25]. Overexpression of miR185-5p induced collagen production and pro-fibrosis activation in cardiac fibroblasts, and promoted cardiac interstitial fibrosis [34]. Overexpression of miR-185-5p significantly inhibited VEGFA to improve ovarian morphological damage and angiogenesis in rats with polycystic ovary syndrome [35]. Pang et al. [36] demonstrated that miR-185-5p restricted acute myeloid leukemia cells proliferation and invasion, enhanced cell differentiates and apoptosis.

ATG101 is located on human chromosome 12 q13.13, is an important component of the eukaryotic ULK1 autophagy initiation complex and participates in autophagy by forming a stable complex with ULK1-ATG12-FIP200, as well as play an important role in recruiting autophagy downstream molecules [38]. ATG101 has been demonstrated to mediate autophagy to regulate the process of myocardial oxidative damage [39], pancreatic cancer [40], and maintain neuronal and midgut homeostasis [41]. Knocking down ATG101 promoted proliferation and limited apoptosis of H<sub>2</sub>O<sub>2</sub>-stimulated mouse neonatal cardiomyocytes by dampening autophagy [39]. Downregulation of ATG101 increased the apoptosis of human pulmonary arterial endothelial cells, attenuated autophagy and proliferation ability, and may acted as a potential therapeutic target of disease involving endothelial injury [42]. In the present study, we illustrated that ATG101 was a target of miR-185-5p, and miR-185-5p negatively regulated ATG101 expression. Increased ATG101 activated autophagy markers ATG5, ATG12, LC3II/I, Beclin1 and tight junction-associated proteins ZO1, Occludin, E-cadherin,  $\beta$ -catenin expression, upregulated the numbers of autophagosomes and the values of TEER, dampened the flux of FITC-dextran in OGD/R-induced Caco-2 cells. Overexpression of miR-185-5p reversed the effect of overexpressed ATG101 on Caco-2 cells.

In conclusion, miR-185-5p expression in OGD/R-stimulated Caco-2 cells and II/R mice was rose. Inhibited miR-185-5p promoted ATG101 expression, protected the intestinal barrier and alleviated intestinal damage by upregulating autophagy level. Contrary, overexpression of miR-185-5p disrupted tight junction and aggravated intestinal damage by decreased autophagy level. As a new diagnosis and treatment strategy for autophagy-mediated II/R injury, the miR-185-5p/ATG101 axis has important research value.

#### Ethics statement

This study was approved by the Laboratory Animal Ethics Committee of Yunnan Laberal Biotechnology co., Ltd (PZ20220413).

#### Author contribution statement

Wendong Chen: Conceived and designed the experiments; Wrote the paper.

Li Ma, Chun Bi: Analyzed and interpreted the data; Contributed reagents, materials, analysis tools or data.

Jianlin Shao: Contributed reagents, materials, analysis tools or data; Wrote the paper.

Junjie Li: Performed the experiments.

Wei Yang: Conceived and designed the experiments; Contributed reagents, materials, analysis tools or data.

#### Funding statement

Wendong Chen was supported by Yunnan health training project of high-level talents {H-2019028}.

#### Data availability statement

Data included in article/supplementary material/referenced in article.

#### Declaration of competing interest

The authors declare that they have no known competing financial interests or personal relationships that could have appeared to influence the work reported in this paper.

#### Appendix A. Supplementary data

Supplementary data to this article can be found online at <https://doi.org/10.1016/j.heliyon.2023.e18325>.



## References

- [1] Y.L. Wong, I. Lautenschläger, L. Hummitzsch, et al., Effects of different ischemic preconditioning strategies on physiological and cellular mechanisms of intestinal ischemia/reperfusion injury: implication from an isolated perfused rat small intestine model[J], *PLoS One* 16 (9) (2021), e0256957.
- [2] T. Kalogeris, C.P. Baines, M. Krenz, et al., Ischemia/Reperfusion[J], *Compr. Physiol.* 7 (1) (2016) 113–170.
- [3] M. Mura, C.F. Andrade, B. Han, et al., Intestinal ischemia-reperfusion-induced acute lung injury and oncotic cell death in multiple organs[J], *Shock* 28 (2) (2007) 227–238.
- [4] A. Pierro, S. Eaton, Intestinal ischemia reperfusion injury and multisystem organ failure[J], *Semin. Pediatr. Surg.* 13 (1) (2004) 11–17.
- [5] L. Liu, J. Yao, Z. Li, et al., miR-381-3p knockdown improves intestinal epithelial proliferation and barrier function after intestinal ischemia/reperfusion injury by targeting nurr1[J], *Cell Death Dis.* 9 (3) (2018) 411.
- [6] T. Suzuki, Regulation of the intestinal barrier by nutrients: the role of tight junctions[J], *Anim. Sci. J.* 91 (1) (2020), e13357.
- [7] L.W. Kaminsky, R. Al-Sadi, T.Y. Ma, IL-1 $\beta$  and the intestinal epithelial tight junction barrier[J], *Front. Immunol.* 12 (2021), 767456.
- [8] Y.B. Yu, D.Y. Zhao, Q.Q. Qi, et al., BDNF modulates intestinal barrier integrity through regulating the expression of tight junction proteins[J], *Neuro Gastroenterol. Motil.* 29 (3) (2017).
- [9] L.P. Bharath, M. Agrawal, G. Mccambridge, et al., Metformin enhances autophagy and normalizes mitochondrial function to alleviate aging-associated inflammation[J], *Cell Metabol.* 32 (1) (2020) 44–55.e6.
- [10] B.N. Lizama, C.T. Chu, Neuronal autophagy and mitophagy in Parkinson's disease[J], *Mol. Aspect. Med.* 82 (2021), 100972.
- [11] X. Li, S. He, B. Ma, Autophagy and autophagy-related proteins in cancer[J], *Mol. Cancer* 19 (1) (2020) 12.
- [12] L. Feng, Z. Yang, Y. Li, et al., MicroRNA-378 contributes to osteoarthritis by regulating chondrocyte autophagy and bone marrow mesenchymal stem cell chondrogenesis[J], *Mol. Ther. Nucleic Acids* 28 (2022) 328–341.
- [13] M.L. Chen, C.G. Hong, T. Yue, et al., Inhibition of miR-331-3p and miR-9-5p ameliorates Alzheimer's disease by enhancing autophagy[J], *Theranostics* 11 (5) (2021) 2395–2409.
- [14] X. Peng, Y. Wang, H. Li, et al., ATG5-mediated autophagy suppresses NF- $\kappa$ B signaling to limit epithelial inflammatory response to kidney injury[J], *Cell Death Dis.* 10 (4) (2019) 253.
- [15] Y. Zhang, X. Li, Y. Li, et al., DNA damage-regulated autophagy modulator 1 (DRAM1) mediates autophagy and apoptosis of intestinal epithelial cells in inflammatory bowel disease[J], *Dig. Dis. Sci.* 66 (10) (2021) 3375–3390.
- [16] Z. Liu, K. Hu, Y.S. Chen, et al., JAK2/STAT3 inhibition attenuates intestinal ischemia-reperfusion injury via promoting autophagy: in vitro and in vivo study[J], *Mol. Biol. Rep.* 49 (4) (2022) 2857–2867.
- [17] L. Zhenzhen, L. Wenting, Z. Jianmin, et al., miR-146a-5p/TXNIP axis attenuates intestinal ischemia-reperfusion injury by inhibiting autophagy via the PRKAA/mTOR signaling pathway[J], *Biochem. Pharmacol.* 197 (2022), 114839.
- [18] R. Chen, Y.Y. Zhang, J.N. Lan, et al., Ischemic preconditioning alleviates intestinal ischemia-reperfusion injury by enhancing autophagy and suppressing oxidative stress through the akt/GSK-3 $\beta$ /nrf2 pathway in mice[J], *Oxid. Med. Cell. Longev.* 2020 (2020), 6954764.
- [19] Y. Li, Y. Luo, B. Li, et al., miRNA-182/Deptor/mTOR axis regulates autophagy to reduce intestinal ischaemia/reperfusion injury[J], *J. Cell Mol. Med.* 24 (14) (2020) 7873–7883.
- [20] X. Pei, S.W. Chen, X. Long, et al., circMET promotes NSCLC cell proliferation, metastasis, and immune evasion by regulating the miR-145-5p/CXCL3 axis[J], *Aging (Albany NY)* 12 (13) (2020) 13038–13058.
- [21] Y. Chen, W. Liao, A. Yuan, et al., MiR-181a reduces radiosensitivity of non-small-cell lung cancer via inhibiting PTEN[J], *Panminerva Med.* 64 (3) (2022) 374–383.
- [22] F. Zhou, Y.K. Wang, C.G. Zhang, et al., miR-19a/b-3p promotes inflammation during cerebral ischemia/reperfusion injury via SIRT1/FoxO3/SPHK1 pathway [J], *J. Neuroinflammation* 18 (1) (2021) 122.
- [23] X. Ma, H. Liu, J. Zhu, et al., miR-185-5p regulates inflammation and phagocytosis through CDC42/JNK pathway in macrophages[J], *Genes* 13 (3) (2022) 468.
- [24] D. Zhao, J. Guo, L. Liu, et al., Rosiglitazone attenuates high glucose-induced proliferation, inflammation, oxidative stress and extracellular matrix accumulation in mouse mesangial cells through the Gm26917/miR-185-5p pathway[J], *Endocr. J.* 68 (7) (2021) 751–762.
- [25] J. Sun, Y.M. Zhu, Q. Liu, et al., LncRNA ROR modulates myocardial ischemia-reperfusion injury mediated by the miR-185-5p/CDK6 axis[J], *Lab. Invest.* 102 (5) (2022) 505–514.
- [26] Y. Yang, X.R. Liu, Z. Jin, [Effects of interference with UCA1 and inhibition of miR-185-5p on activation, autophagy and survival of  $\beta$ -catenin pathway in non-small cell lung cancer][J], *Sichuan Da Xue Xue Bao Yi Xue Ban* 50 (2) (2019) 157–163.
- [27] C. Liu, L. Ji, X. Song, Long non coding RNA UCA1 contributes to the autophagy and survival of colorectal cancer cells via sponging miR-185-5p to up-regulate the WSP2/ $\beta$ -catenin pathway[J], *RSC Adv.* 9 (25) (2019) 14160–14166.
- [28] C.A. Hu, Y. Hou, D. Yi, et al., Autophagy and tight junction proteins in the intestine and intestinal diseases[J], *Anim Nutr* 1 (3) (2015) 123–127.
- [29] L.X. Li, L.H. Yin, M. Gao, et al., MiR-23a-5p exacerbates intestinal ischemia-reperfusion injury by promoting oxidative stress via targeting PPAR alpha[J], *Biochem. Pharmacol.* 180 (2020), 114194.
- [30] Z. Jia, W. Lian, H. Shi, et al., Ischemic preconditioning protects against intestinal ischemia/reperfusion injury via the HIF-1 $\alpha$ /miR-21 Axis[J], *Sci. Rep.* 7 (1) (2017), 16190.
- [31] Z. Li, G. Wang, D. Feng, et al., Targeting the miR-665-3p-ATG4B-autophagy axis relieves inflammation and apoptosis in intestinal ischemia/reperfusion[J], *Cell Death Dis.* 9 (5) (2018) 483.
- [32] G. Wang, J. Yao, Z. Li, et al., miR-34a-5p inhibition alleviates intestinal ischemia/reperfusion-induced reactive oxygen species accumulation and apoptosis via activation of SIRT1 signaling[J], *Antioxid. Redox Signal.* 24 (17) (2016) 961–973.
- [33] L. Zheng, X. Han, Y. Hu, et al., Dioscin ameliorates intestinal ischemia/reperfusion injury via adjusting miR-351-5p/MAPK13-mediated inflammation and apoptosis[J], *Pharmacol. Res.* 139 (2019) 431–439.
- [34] R. Lin, L. Rahtu-Korpela, Z. Szabo, et al., MiR-185-5p regulates the development of myocardial fibrosis[J], *J. Mol. Cell. Cardiol.* 165 (2022) 130–140.
- [35] J. Wei, Y. Zhao, MiR-185-5p protects against angiogenesis in polycystic ovary syndrome by targeting VEGFA[J], *Front. Pharmacol.* 11 (2020) 1030.
- [36] B. Pang, H. Mao, J. Wang, et al., MiR-185-5p suppresses acute myeloid leukemia by inhibiting GPX1[J], *Microvasc. Res.* 140 (2022), 104296.
- [37] X. Ma, H. Liu, J. Zhu, et al., miR-185-5p regulates inflammation and phagocytosis through CDC42/JNK pathway in macrophages[J], *Genes* 13 (3) (2022).
- [38] J. Ma, Y. Yang, J. Han, Research progress of new autophagy-related protein Atg101[J], *Chin. J. Cell Biol.* 42 (3) (2020) 507–511.
- [39] J. Zhou, L. Li, H. Hu, et al., Circ-HIPK2 accelerates cell apoptosis and autophagy in myocardial oxidative injury by sponging miR-485-5p and targeting ATG101 [J], *J. Cardiovasc. Pharmacol.* 76 (4) (2020) 427–436.
- [40] J. Lee, J. Kim, J. Shin, et al., ATG101 degradation by HUWE1-mediated ubiquitination impairs autophagy and reduces survival in cancer cells[J], *Int. J. Mol. Sci.* 22 (17) (2021) 9182.
- [41] T. Guo, Z. Nan, C. Miao, et al., The autophagy-related gene Atg101 in Drosophila regulates both neuron and midgut homeostasis[J], *J. Biol. Chem.* 294 (14) (2019) 5666–5676.
- [42] J. Du, Z. Xu, Q. Liu, et al., ATG101 single-stranded antisense RNA-loaded triangular DNA nanoparticles control human pulmonary endothelial growth via regulation of cell macroautophagy[J], *ACS Appl. Mater. Interfaces* 9 (49) (2017) 42544–42555.